Experimental Investigation on Effect of Fin Height on Microscale Heat Transfer and Fluid Flow for Macro Scale Industrial Applications

Cheng, Kai Xian; Goh, Aik Ling; Hadi, Mulyadi; Ooi, Kim Tiow

2017

Cheng, K. X., Goh, A. L., Hadi, M., & Ooi, K. T. (2017). Experimental Investigation on Effect of Fin Height on Microscale Heat Transfer and Fluid Flow for Macro Scale Industrial Applications. IOP Conference Series: Materials Science and Engineering, 187, 012003-.

https://hdl.handle.net/10356/83606

https://doi.org/10.1088/1757-899X/187/1/012003

Experimental Investigation on Effect of Fin Height on Microscale Heat Transfer and Fluid Flow for Macro Scale Industrial Applications

K X Cheng[1], A L Goh[1], M Hadi[1], K T Ooi[1]

[1] School of Mechanical and Aerospace Engineering, Nanyang Technological University, 50 Nanyang Avenue, Singapore 639798.

Abstract. Microchannel for macro geometry application is gaining popularity particularly in aerospace, biomedical and photovoltaic. A novel method of employing microchannel in macro geometry at lower cost using conventional machining methods has been developed. A solid cylinder on outer diameter 19.4 mm is placed concentrically into a copper pipe of inner diameter 20 mm, forming an annular microchannel with 300 μm gap. This study takes a step further by introducing surface profile of different heights on the surface of solid cylinder and investigating the effect on two main design objectives- increasing heat removal capability at same pumping power and reducing pumping power for the same heat removal duty. Four surface profiles -parallel fins as well as fins with height of 0.1, 0.2 and 0.3 mm, were investigated experimentally at constant heat flux at Reynolds number from 690 to 4600. The amount of fluid in the microchannel, channel length of 30 mm, bifurcating angle of 75 degrees and mean hydraulic diameter of 600 μm are kept as constant parameters. A plain insert is used as benchmark for comparison of enhancement. In this study, insert with fins of 0.3 mm attains the highest enhancement of 43 percent increment in heat transfer as compared to plain insert using the same pumping power. While keeping the heat removal duty constant, the same insert is able to perform the duty using less than 50 percent the pumping power required by the plain insert at low Reynolds numbers.

1. Introduction

Single-phase heat transfer and fluid flow in microscale channels have been an active research regime since 1981. Tuckerman and Pease [1] first implemented microscale heat sink for silicon integrated circuit. Their work has then spurred numerous works on microchannel which can be categorised into design and implementation, fundamental understanding and classification and practical implementation with enhancement for the next few decades, as reported by Kandlikar [2]. Goodling [3], Sobhan and Garimella [4], Palm [5] and Mohammed [6] have done excellent reviews on this topic.

Kandlikar [7] summarised the works up to 2012 and highlighted the research needs for the implementation of microchannel in heat exchangers. Kong and Ooi [8] made a paradigm shift in the implementation of microscale heat transfer in macro geometry in 2013. An annular channel with a microscale gap of 300 μm was created by inserting a solid cylinder of mean diameter 19.4 mm concentrically into another hollow cylinder of inner diameter 20 mm. The research demonstrated the feasibility of the implementation of microscale heat transfer in macro scale system at a relatively low cost as the system was manufactured through conventional machining processes, instead of the complex and costly microfabrication techniques.

Goh and Ooi [9] further improved the thermal performance of the system by implementing surface profile on the inner solid cylinder. The nature-inspired inverted fish scale profile enhanced the overall thermal performance, citing re-initialisation of boundary layers, flow recirculation and higher turbulence intensity as the possible reasons. Nonetheless, less attention was paid on the fluid flow in order to attempt the high pressure drop woes.

Other studies looked into reducing pressure drop in conventional microchannels. Lorenzini and Kandlikar [10] studied numerically the effect of introducing fins of variable density along the length of the microchannel. The work draw attention to pressure drop issue on top of thermal performance of the channel by considering the coefficient of performance. Wang et al. [11] examined tree and leaf-like network in terms of thermal and hydrodynamic performance. Their work highlighted the role of bifurcation in recovering the local pressure drop.

Hence this project takes previous work done by Goh and Ooi [9] to a step further by implementing fins on the surface of the inner cylinder to reduce the overall pressure drop. This study hypothesises that flow bifurcation aids in recovering local pressure while the fins keep the flow within the developing region along the length of the microchannel. This project experimentally investigates three different fin heights and the effect on the thermal and hydrodynamic performance, using a plain profile as the reference. The heat transfer area, total amount of heat supply, average channel gap size, channel length and degree of bifurcation are kept constant in this study.

2. Experimental setup and procedures

2.1. Experimental setup

Figure 1 shows the experimental setup used in this study. The chiller, bypass loop, filter, test loop, measuring devices, test module and data acquisition system are the key components of the setup.

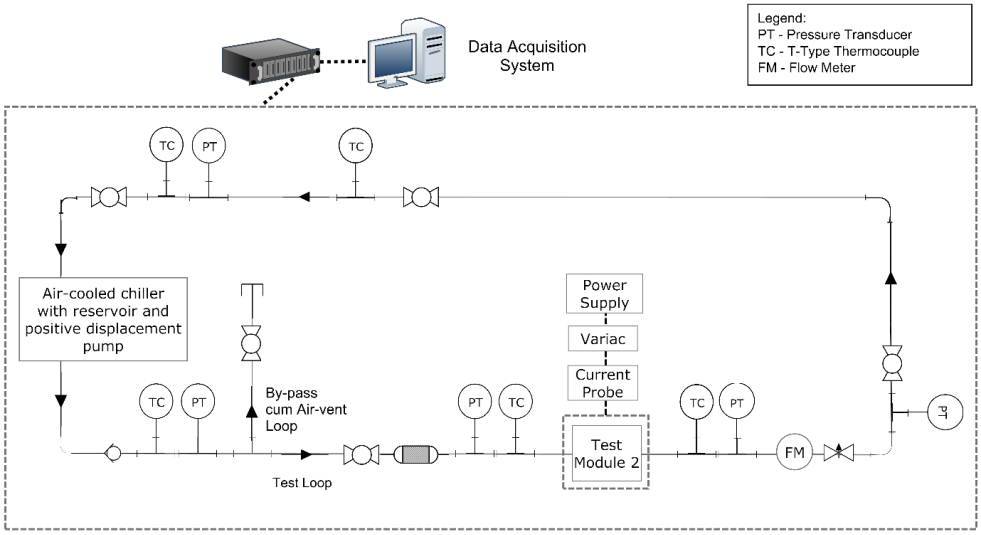

Figure 1: Experimental test bed

The working fluid is water and it is stored in the reservoir. It is recirculated and cooled to the desired inlet temperature and pumped into the test loop by a positive displacement pump integrated within the chiller. The volumetric flow of the water is controlled by a bypass loop and a needle valve located downstream of the test module. The air-vent loop serves to remove air bubbles trapped in the test loop.

The water is first channeled through a 40-micron filter to remove solid particles before entering the test loop. The flow conditions including the fluid temperature and pressure are monitored by a T-type thermocouples and pressure transducers respectively, along the test loop. The heat generated by the

test module is removed by water which will be channeled back to the reservoir thereafter for recirculation.

2.2. Experimental test module

Figure 2 and **Figure 3** illustrate sectional view and side view of the test module respectively. An insert of a nominal diameter of 19.4 mm is placed concentrically into the copper block with an inner diameter of 20 mm, forming an annular channel of 0.6 mm width. Essentially, a 300 µm microchannel is formed within the test module as highlighted in **Figure 3**.

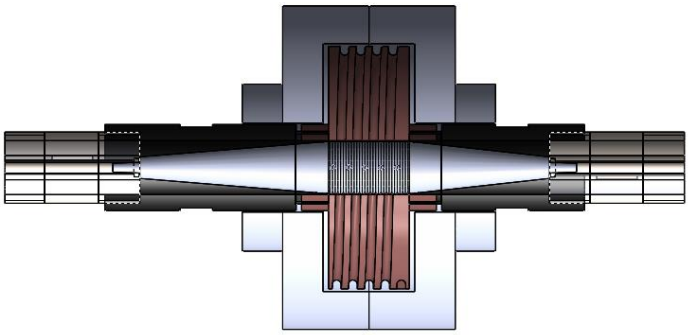

Figure 2: Sectional view of the test module

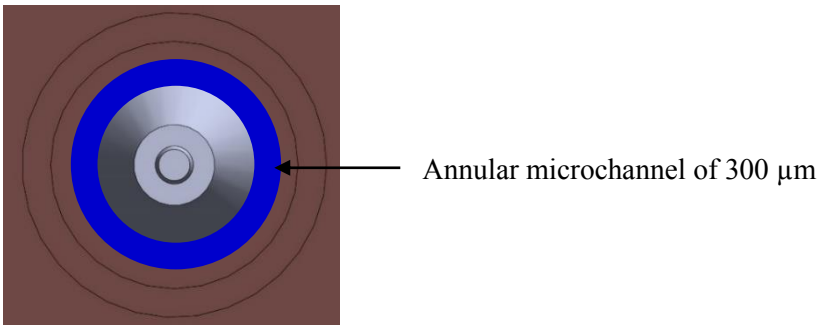

Figure 3: Side view of test module

2.3. Insert Design

A total of five inserts are investigated experimentally in this study, namely plain, parallel-fin, fin_1, fin_2 and fin_3 inserts. **Figure 4**, **Figure 5** and **Figure 6** illustrate plain, parallel-fin and fin_1 insert respectively. Fin_1, fin_2 and fin_3 have 75 degree bifurcating fins on the surface of the insert with three different heights of 0.1 mm, 0.2 mm and 0.3 mm. The height of the fin is depicted in **Figure 7**. The parallel-fin insert has a fin height of 0.2 mm. All the inserts have a nominal diameter of 19.4 mm in the heating region to ensure constant amount of fluid in the microchannel.

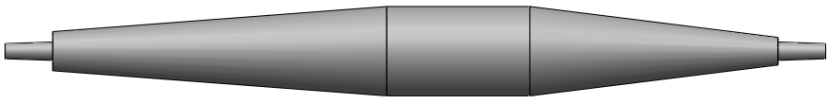

Figure 4: Plain insert

Figure 5: Parallel-fin insert

Figure 6: cfin_1 insert

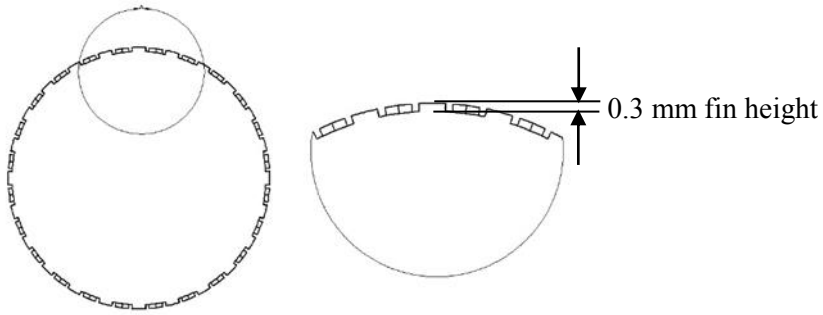

(a) (b)

Figure 7: (a) Side view of the portion of the insert within the heating region; (b) magnified view of the portion highlighted by circle

2.4. Measuring devices

J- and T-type thermocouples are used to measure water temperature in the experimental setup. A total of five T-type thermocouples are used. Two of them are installed before and after the test module while the other three are installed along the flow loop for monitoring purposes. A total of twelve J-type thermocouples are incorporated into the test module. Five of these thermocouples are installed on each side of the test module, 2.5 mm radially away from the wall of the microchannel to acquire readings for the computation of wall temperature. The other two are placed 5 mm from the outer surface of the test module, sending signal to data acquisition system and circuit breaker for safety reasons.

WIKA model A-10 pressure transducers are used to monitor the pressure in the system, giving current signals of 4 to 20 mA which correspond to pressure readings of 0 to 6 barg. Two of the pressure transducers are installed before and after the test module while the other three are positioned along the flow loop for monitoring purposes. The flow rate is measured by a Coriolis mass flow meter.

2.5. Data reduction

The data acquired during the 10-minute steady state condition is processed to obtain thermal and hydrodynamic parameters.

The heat transfer coefficient, h is obtained from Newton's law of cooling as shown in Equation (1).

$$h = \frac{\dot{Q}}{A\left(T_{w,m} - T_{f,m}\right)} \tag{1}$$

The rate of heat transferred to the fluid, $\dot{Q}$ is deduced from the inlet and outlet fluid temperatures as shown in Equation (2). The mass flow rate, $\dot{m}$ is the product of temperature-dependent density and volumetric flow rate. All the fluid properties are obtained from National Institute of Standards and Technology (NIST) Reference Fluid and Thermodynamic and Transport Properties Database (REFPROP).

$$\dot{Q} = \dot{m} c_{p,m} \left(T_{out} - T_{in}\right) \tag{2}$$

The heat transfer area is kept constant at 1885 mm^2. The fluid temperature, is computed by taking the average of the inlet and outlet fluid temperature, as shown in Equation (3).

$$T_{f,m} = \frac{T_{in} + T_{out}}{2} \tag{3}$$

The wall temperature, on the other hand, is deduced from J-type thermocouples. The thermal resistance of the copper block in the radial direction is taken into account to get the wall temperature as depicted in Equation (4).

$$T_{w,i} = T_{r,i} - q\frac{\ln\left(d_r / d_w\right)}{2\pi L k_c} \tag{4}$$

The wall temperature is therefore assumed to be the average of the ten points along the wall of the copper block, according to Equation (5).

$$T_{w,m} = \left(\sum_{i=1}^{10} T_{w,i}\right) / 10 \tag{5}$$

Equation (6) and (7) are used to compute Nusselt number and Reynolds number respectively.

$$Nu = \frac{hD_h}{k_f} \tag{6}$$

$$\mathrm{Re} = \frac{\dot{m}D_h}{A_c \mu} \tag{7}$$

The pressure drop is deduced from the pressure difference between the inlet and outlet of the test module as shown in Equation (8).

$$\Delta P = P_{in} - P_{out} \tag{8}$$

Performance evaluation criteria for two main objectives of the design: increased heat duty for equal pumping power and reduced pumping power for constant heat duty, were introduced by Webb [12-14]. The subscript s stands for smooth surface or plain insert for our case. Equation (9) is the objective function for increased heat duty at the same pumping power while Equation (10) evaluates the performance aimed at reducing pumping power for the same heat duty.

$$\frac{UA}{U_s A_s} = \frac{Nu / Nu_s}{\left(\Delta P / \Delta P_s\right)^{1/3}} \tag{9}$$

$$\frac{P}{P_s} = \frac{\Delta P / \Delta P_s}{\left(Nu / Nu_s\right)^3} \tag{10}$$

2.6. Experimental operating conditions

The study was conducted for Reynolds number from 690 to 4600 with a constant heat supply of 500 W. The heat supply area was kept constant at 18.85 cm^2.

3. Results and Discussion

Figure 8 shows the convective heat transfer coefficient for all the inserts. The highest heat transfer coefficient obtained for the study is 45.0 $kW/m^2 \cdot K$ using fin_3 insert at a Reynolds number of 4563. This is equivalent to a Nusselt number of 42.46.

It is obvious from **Figure 8** that all the inserts with fins achieve higher heat transfer coefficients as compared to plain insert. Fin_3 yields the highest heat transfer coefficients at all Reynolds numbers, This is probably due to the lowest minimum gap size between the fin and the wall despite the constant nominal diameter. Nonetheless, fin_3 results in higher pressure drop at all flow rates as depicted in **Figure 9**. Although the pressure drop is relatively high at higher Reynolds numbers especially for fin_3 insert, the pumping requirement can be easily met by a commercially readily available pump.

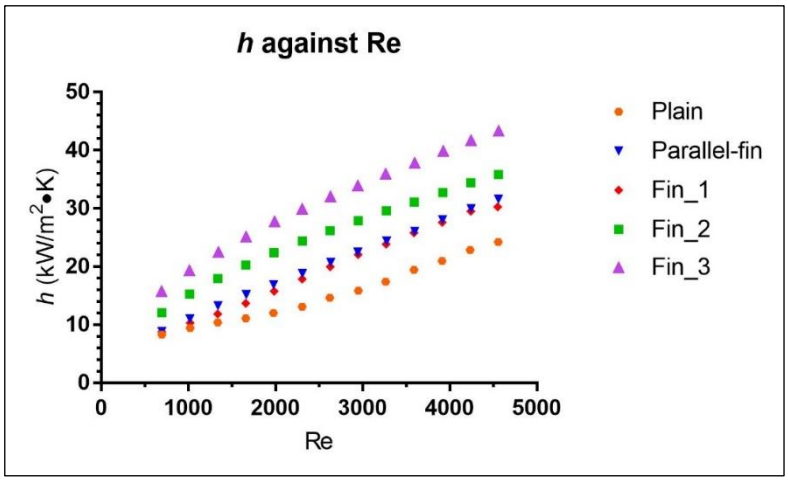

Figure 8: Heat transfer coefficient against Reynolds number

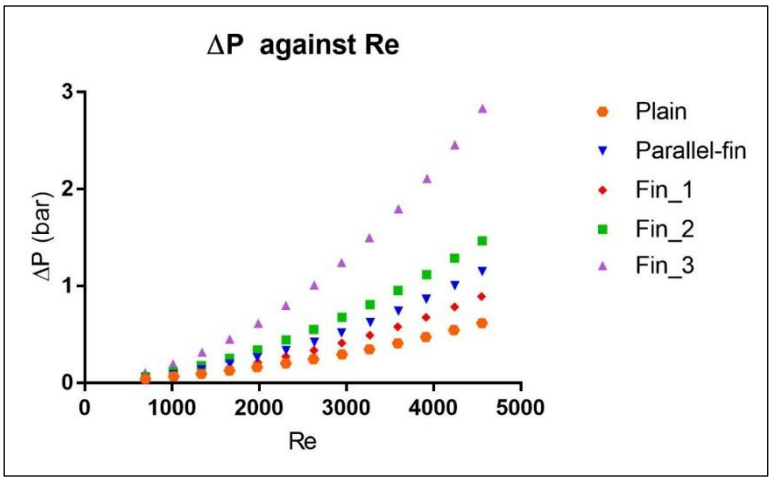

Figure 9: Pressure drop against Reynolds number

Figure 10 compares the performance of all the inserts against the plain insert, aiming to incearse the heat removal capability at the same pumping power. The highest index achieved is 1.48, and it is by fin_3 insert at Reynolds number from 1660 to 2000. On the other hand, fin_2 depicts similar performance index particularly at high Reynolds number. At low Reynolds number, fin_3 slightly out performs fin_2 insert. This is likely due to smaller minimum gaps formed by fin_3 might have initiated higher turbulence as compared to those of fin_2. Notably, the transition Reynolds number is around 2000, which is close enough to the critical Reynolds number for conventionally sized channels of 2300. Interestingly, both parallel-fin and fin_1 inserts have similar performance index despite having differing surface profile. The re-initilisation of boundary layers along the length of the channel by the discontinuous surface profile on fin_1 insert might have compensated for the larger minimum gaps as compared to those of the parallel-fin insert which has a higher fin height at 0.2 mm. It is obvious that- channels with a higher fin height show higher heat removal capability especially at low Reynolds numbers.

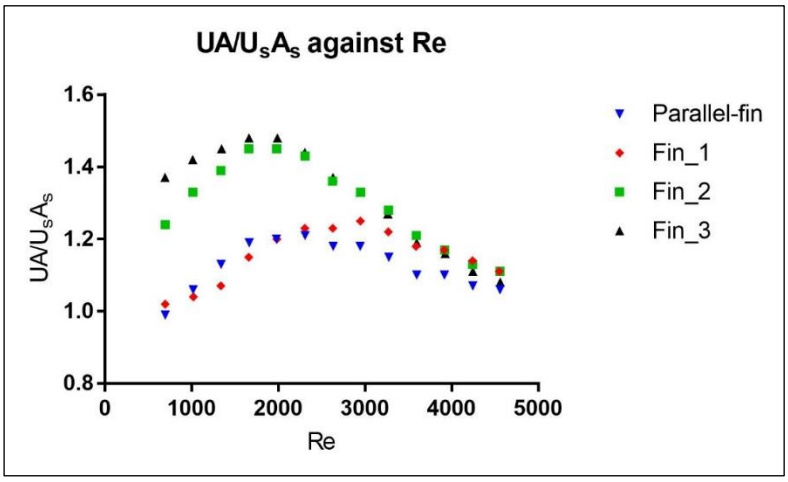

Figure 10: UA/U_sA_s against Reynolds number

Figure 11 shows the plot of performance index which aims at reducing pumping power but keeping heat removal capability constant. Although all the inserts have similar low pressure drop at low Reynolds as shown in **Figure 9**, this phenomenon is accompanied by low heat removal ability for parallel-fin and fin_1 inserts. Therefore, both inserts have a relatively high performance index. The fin_2 and fin_3 account for the slightly higher pressure drop at low Reynolds number by much higher thermal performance, requiring less than 50 percent of the pumping power as compared to the plain insert to achieve the same heat removal duty. Similar to the performance index for heat removal capability, all the inserts have close index for pumping power requirement at high Reynolds number. However, it is obvious that all the inserts have an index less than 1, implying that the surface profiles actually lower the pumping power for the same heat removal capability. The results show that both performance indices for heat duty and pumping power are the most ideal near to Reynolds number of 2000.

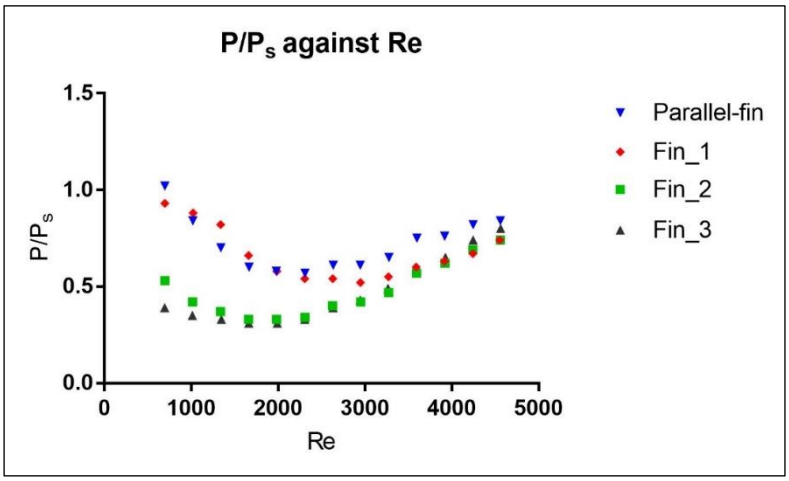

Figure 11:P/P_s against Reynolds number

4. Conclusion

a. This study demonstrates the feasibility of enhancing the thermal and hydrodynamic performance of microchannel in macro geometry using surface profiles. It shows that bifurcating fins perform better than parallel fins both in heat transfer capability and pressure drop.

b. For the same pumping power, a higher fin enhances heat transfer more than the shorter fin, particularly at low Reynolds numbers. The highest enhancement of 43 % in heat transfer as compared to plain insert is achieved by fin_3 at a Reynolds number close to 2000.
c. Considering the same amount of heat being removed, all the surface profiles require less pumping power as compared to plain insert. Both fin_2 and fin_3 need less than half the pumping power required by plain insert to remove the same amount of heat at low Reynolds numbers.

The findings from this study can be used a reference for further studies on the microchannel enhancement in macro geometries as fin height plays significant role both in terms of heat transfer and pressure drop issue.

5. References

[1] Tuckerman, D.B. and R. Pease, *High-performance heat sinking for VLSI.* IEEE Electron device letters, 1981. **2**(5): p. 126-129.
[2] Kandlikar, S.G., History, advances, and challenges in liquid flow and flow boiling heat transfer in microchannels: a critical review. Journal of Heat Transfer, 2012. **134**(3): p. 034001.
[3] Goodling, J.S. Microchannel heat exchangers: A review. in SPIE's 1993 International Symposium on Optics, Imaging, and Instrumentation. 1993. International Society for Optics and Photonics.
[4] Sobhan, C.B. and S.V. Garimella, *A comparative analysis of studies on heat transfer and fluid flow in microchannels.* Microscale Thermophysical Engineering, 2001. **5**(4): p. 293-311.
[5] Palm, B., *Heat transfer in microchannels.* Microscale Thermophysical Engineering, 2001. **5**(3): p. 155-175.
[6] Mohammed, H., et al., Heat transfer and fluid flow characteristics in microchannels heat exchanger using nanofluids: a review. Renewable and Sustainable Energy Reviews, 2011. **15**(3): p. 1502-1512.
[7] Kandlikar, S.G., et al., *Heat transfer in microchannels—2012 status and research needs.* Journal of Heat Transfer, 2013. **135**(9): p. 091001.
[8] Kong, K.S. and K.T. Ooi, A numerical and experimental investigation on microscale heat transfer effect in the combined entry region in macro geometries. International Journal of Thermal Sciences, 2013. **68**: p. 8-19.
[9] Goh, A.L. and K.T. Ooi, *Nature-inspired Inverted Fish Scale microscale passages for enhanced heat transfer.* International Journal of Thermal Sciences, 2016. **106**: p. 18-31.
[10] Lorenzini-Gutierrez, D. and S.G. Kandlikar, Variable Fin Density Flow Channels for Effective Cooling and Mitigation of Temperature Nonuniformity in Three-Dimensional Integrated Circuits. Journal of Electronic Packaging, 2014. **136**(2): p. 021007-021007.
[11] Wang, X.-Q., et al., *Flow and thermal characteristics of offset branching network.* International Journal of Thermal Sciences, 2010. **49**(2): p. 272-280.
[12] Webb, R., Performance evaluation criteria for use of enhanced heat transfer surfaces in heat exchanger design. International Journal of Heat and Mass Transfer, 1981. **24**(4): p. 715-726.
[13] Webb, R. and M. Scott, A parametric analysis of the performance of internally finned tubes for heat exchanger application. Journal of Heat Transfer, 1980. **102**(1): p. 38-43.
[14] Gee, D.L. and R. Webb, *Forced convection heat transfer in helically rib-roughened tubes.* International Journal of Heat and Mass Transfer, 1980. **23**(8): p. 1127-1136.